Neurobiology of Stress 13 (2020) 100233

Contents lists available at ScienceDirect

Neurobiology of Stress

journal homepage: www.elsevier.com/locate/ynstr

Functional networks activated by controllable and uncontrollable stress in male and female rats

N.B. Worley, Ph.D. *, S.R. Everett, A.R. Foilb, Ph.D., J.P. Christianson, Ph.D.

Department of Psychology, Boston College, Chestnut Hill, MA, 02467, USA

ARTICLE INFO

Keywords:
Stressor controllability
Sex differences
Network analysis
Fos
Action-outcome

ABSTRACT

The ability of an individual to reduce the intensity, duration or frequency of a stressor is a critical determinant of the consequences of that stressor on physiology and behavior. To expand our understanding of the brain networks engaged during controllable and uncontrollable stress and to identify sex differences, we used functional connectivity analyses of the immediate early gene product Fos in male and female rats exposed to either controllable or uncontrollable tail shocks. Twenty-eight regions of interest (ROI) were selected from the structures previously evinced to be responsible for stress response, action-outcome learning, or sexual dimorphism. We found that connectivity across these structures was strongest in female rats without control while weaker connectivity was evident in male rats with control over stress. Interestingly, this pattern correlates with known behavioral sex differences where stressor controllability leads to resilience in male but not female rats. Graph theoretical analysis identified several structures important to networks under specific conditions. In sum, the findings suggest that control over stress reshapes functional connectivity.

1. Introduction

1.1. Stress and coping

Stress is a risk factor for neuropsychiatric disorders such as post-traumatic stress disorder and depression (Gillikin et al., 2016), yet not all individuals exposed to stress develop such disorders. Coping strategy is one of several factors that influence susceptibility versus resilience to the effects of stress. In both humans and laboratory rodents, active coping strategies correlate with resilience (Maier and Watkins, 2005; Southwick et al., 2005; Thompson et al., 2018). Biological sex is another predictor of susceptibility to stress as women are more likely to develop a stress related neuropsychiatric disorder following acute stress exposure (Valentino and Bangasser, 2016) or experience depression and anxiety disorders across the lifetime (Breslau; Naomi, 2002; Breslau and Davis, 1992). A better understanding of the neural basis of coping, and how it varies by sex, is needed to develop more effective and equitable strategies for treating and preventing stress related disorders.

Research in rodents using the stressor controllability paradigm allows the direct comparison of the neurobiology and behavior of a rat given behavioral control over the termination of a stressor, referred to as escapable stress (ES), to a yoked partner without control over the stressor, referred to as inescapable stress (IS) (Maier and Seligman, 2016). This procedure is very useful in the study of coping because in male rats, IS causes a constellation of behavioral changes that appear to be homologous to stressor induced behaviors observed in humans (Herbison et al., 2017). Specifically, IS leads to failure to escape in a shuttle box, exaggerated fear conditioning, and reduced social interaction with a juvenile conspecific (Christianson et al., 2010; Maier, 1990; Maier and Seligman, 2016; Short and Maier, 1993). Coping is critical because none of these changes occur in rats with control over the stressor.

In the stressor controllability paradigm, the effects of IS on later behaviors are dependent on serotonin neurons in the dorsal raphe nucleus (DRN) that are sensitized by IS causing these neurons to release high levels of 5-HT in regions proximal to the control of affect and anxiety, such as the basolateral amygdala (Christianson et al., 2010). When a rat has control over stress, on the other hand, sensitization of the 5-HT system is prevented through the activation of prelimbic cortex (PL) that projects to the raphe and inhibits 5-HT activity during stress (Amat et al., 2005; Baratta et al., 2018); for reviews see (Christianson and Greenwood, 2014; Maier and Watkins, 2010; Worley et al., 2018).

Research seeking to understand stress resilience in females reveals stark contrasts to the behavioral and neurobiological phenotypes of

* Corresponding author. Department of Psychology, Boston College, McGuinn 300, 140 Commonwealth Ave, Chestnut Hill, MA, 02467, USA.
E-mail address: worleyn@bc.edu (N.B. Worley).

https://doi.org/10.1016/j.ynstr.2020.100233
Received 4 March 2020; Received in revised form 3 June 2020; Accepted 5 June 2020
Available online 10 June 2020

male rats. For example, while uncontrollable stress enhanced eye blink conditioning in males, it *reduced* it in females and control over stress in the paradigm reversed this pattern (Leuner et al., 2004). Females receiving ES treatment readily perform the escape behavior (wheel turning) akin to males, but both ES and IS result in exaggerated fear conditioning and reduced social exploration (Baratta et al., 2018), akin to IS effects on males (Christianson et al., 2010; Short and Maier, 1993). Consistent with a lack of behavioral effect of ES, there is no stressor controllability difference in the activation of DRN neurons in females. Accordingly, the PL neurons responsible for inhibition for the DRN in males are not engaged during ES in females (Baratta et al., 2018) and do not exhibit circuit-specific morphological plasticity (Baratta et al., 2019). We believe this finding in the PL-DRN circuit is one of a broader set of sex differences that exist within the neural circuits that are engaged by coping in males and females.

1.2. Goal of current research

The major goal of this study was to begin to describe the neural correlates of active coping and uncontrollable stress at a broad scale in male and female rats. To this end we analyzed Fos expression across a large set of brain regions of interest (ROIs) in male and female rats exposed to either ES or IS. Fos quantification is a high throughput, anatomically precise method to understand both regional and functional connectivity patterns in complex networks that are likely to be engaged during stress (McReynolds et al., 2018) and has been applied in many behavioral settings (Rogers-Carter et al., 2018; Tanimizu et al., 2017; Wheeler et al., 2013). Importantly, Fos has been used to measure neural activity following controllable and uncontrollable stress (Amat et al., 2014; Baratta et al., 2009; Grahn et al., 1999; Machida et al., 2018) allowing for comparison to a significant body of literature. As described below, Fos was analyzed for i.) treatment effects within each ROI, ii.) pairwise correlations of Fos between ROIs to estimate functional connectivity between regions, iii.) graph theory-based network construction and analysis by treatment group. Averages across all ROI pairs or subsets can be compared across treatments to determine group differences in functional connectivity. Selection of ROIs was guided by prior literature in the stressor controllability paradigm and sex differences research which we describe below.

1.3. Region of interest selection

In males, growing evidence suggests that the network responsible for action-outcome learning is recruited during ES. The action-outcome system encodes the relationship between an action and the value of the outcome such that devaluation of the reward reduces responding (Balleine and Dickinson, 1998). Action-outcome learning requires the PL and dorsomedial striatum (DMS) (Corbit and Balleine, 2003; Hart et al., 2018). Importantly, inactivation of either the PL or DMS during ES prevented the development of a stress-resistant behavioral phenotype (Amat et al., 2014, 2005). Thus, we predicted that rats with control over stress would have greater functional connectivity within the action-outcome network which, in addition to the PL and DMS, includes the mediodorsal thalamus, ventral pallidum, nucleus accumbens, ventral tegmental area, and orbitofrontal cortex (Balleine and O'Doherty, 2010). In the current investigation these regions were included and treated as the "action-outcome network" (Table 2).

The negative consequences of IS rely on the DRN, lateral ventral portion of the bed nucleus of the stria terminalis (BNSTlv), and the lateral habenula (LHb, (Amat et al., 2014; Hammack et al., 2004; Maier et al., 1994). Furthermore, lateral septum (LS), nucleus accumbens, periaquiductal gray (PAG), medial preoptic area (MPOA), tenia tecta (DTT), piriform cortex (PIR), and olfactory tubercle (OT) all exhibit some differential activity to uncontrollable stressors (Coco and Weiss, 2005). This set of regions was included in the current study as the "stress network" (Table 2).

Here we exposed male and female rats to either ES or IS following the well-established stressor controllability paradigm (Amat et al., 2005; Baratta et al., 2019, 2009; Christianson et al., 2010; Maier et al., 1994). To characterize the networks activated during controllable or uncontrollable stress, and the influence of sex, we quantified regional Fos levels and interregional correlations to investigate functional connectivity. Next, we generated and compared network parameters using graph theoretical metrics. We found that males exposed to ES had, overall, less functional connectivity than any of the other treatments. The greatest functional connectivity appeared in the IS groups.

2. Methods and materials

2.1. Subjects

Sprague Dawley rats (225–250 g, N = 36 Male; N = 36 Female) were obtained from Envigo (Haslett, Michigan, USA), housed in same-sex pairs, maintained on a 12-h light/dark cycle within the Boston College Animal Care Facility, and allowed 1 week to habituate to their home cages. Although not used in the current analysis, rats received infusions of the retrograde tracer Cholera Toxin b to the PL under isoflurane anesthesia and allowed 2 additional weeks of recovery before stress treatments. All experimental protocols were reviewed and approved by the Boston College Institutional Animal Care and Use Committee (IACUC).

2.2. Stress procedure

For each sex, rats were assigned to one of three groups (ES, IS and HC). The stress procedure involved placing the rat in a wheel turn apparatus (Med Associates Model ENV-586B modified by the insertion of a smooth plexiglass floor) and restraining the tail with cloth tape. Copper electrodes were placed at approximately 2 and 4 cm from the base of the tail, augmented with electrolyte paste and connected to a shocker (Coulbourn Instruments Model H15-13). One hundred tail-shocks were delivered on a variable time schedule with an average intershock interval of 60s. For rats assigned to ES, turning the wheel terminated the shock. Rats rapidly learn this behavior and a progressive fixed ratio (FR) schedule was employed to ensure rats performed an operant response and not simply a reflex. Specifically, each ¼ wheel turn caused the closure of a microswitch, which was detected by a PC running custom software (freely available by contacting the corresponding author). At the outset of the experiment, ¼ wheel turn terminated the shock (FR-1). If the response was made in fewer than 5s then the response doubled on the next trial. This pattern continued until a maximum of 4 full wheel turns was reached (FR-16). Failure (no response in 30s) on any trial reset the escape requirement to FR-1. The rat in the IS condition was physically yoked to the ES subject, but the wheel in the IS box was locked in place and not connected to the computer. This design resulted in yoked pairs of rats with exactly identical exposure to tail shock, with the only difference that the ES subject was able to exert behavioral control over the shock termination. All rats received 1 mA shocks for the first 33 trials, 1.3 mA for the following 33 trails, and 1.6 mA for the remaining 34 trials. Finally, the HC group remained in the colony room until the time of perfusion. This stressor controllability paradigm was chosen because it is exactly the procedure used in a large number of studies by the Maier group (Amat et al., 2014; Baratta et al., 2018, 2009; Christianson et al., 2009, 2008).

2.3. Tissue collection and fos immunohistochemistry procedures

After stress, rats were moved to a quiet room, where they remained undisturbed for 2 h. Rats were perfused with 0.01M heparinized phosphate buffered saline (PBS) followed by 4% paraformaldehyde. Brains were dissected and post-fixed in 4% paraformaldehyde at 4 °C for 24 h before being transferred to 30% sucrose. Brains were then sliced into 40

μm sections at −20 °C and stored in cryoprotectant-filled well plates at 4 °C. The immediate early gene product Fos was identified via immunohistochemistry (IHC) as a neural marker of activation. Fos was visualized as previously, (Rogers-Carter et al., 2018). Free floating sections were blocked with 2% normal donkey serum in PBS-T (0.01% Triton-X100) and incubated overnight in rabbit anti-c-Fos antibody at 1:5000 (Millipore, ABE457). The following morning, sections were washed and incubated in biotinylated donkey anti-rabbit secondary antibody at 1:500 (Jackson ImmunoResearch). Secondary was visualized using the avidin-biotin complex method (ABC Elite Kit, Vector Labs) with chromogen (Vector SG Peroxidase Substrate Kit, Vector Laboratories). At the completion of the reaction, slices were floated onto glass slides, dehydrated, cleared, coverslipped with Permount, and left to dry for 48 h. Sections were imaged at 10× (N.A. = 0.45) objective using a Zeiss AxioImager Z2 light microscope with an AxioCam HRc digital color camera. Fos positive cells were quantified within a standardized area for each region based on atlas images (Paxinos and Watson, 2007). The cell counter plug-in on ImageJ software was used to automate Fos quantification, and parameters were verified by manual cell counts. For each ROI, 2 sections were analyzed bilaterally per animal using a standardized window chosen to fit within each ROI (for window size and shape see Table 1). Counts from ROIs with tissue damage were excluded from analysis. The average of the counts for a given animal was used in later analyses.

2.4. Functional connectivity analyses

Within each of the 4 stressed experimental groups (Male ES, Male IS, Female ES, Females IS) all pairwise correlations between the average number of Fos cells were determined by Pearson correlation coefficient. To investigate effects of stress condition or sex on individual ROI by ROI correlations (i.e. is PL more strongly correlated with DMS in ES versus IS), we contrasted the correlation of each condition to the others (all possible comparisons) using the Fisher r to z transformation and z tests to determine p values for each contrast. The set of p-values were then globally adjusted to correct for multiple comparisons using Benjamini and Hochberg's false discovery rate procedure (Benjamini and Hochberg, 1995) maintaining a false discovery rate of 5%. Pairwise ROI by ROI comparisons identified as significant using this method are summarized in Table 3. To determine how functional connectivity differed by stress condition and sex, we contrasted mean r values for networks selected a priori. The comparisons were i., all regions of interest, ii., the stress network, iii., action-outcome network, and iv., the interaction between stress and action-outcome network. Each comparison was conducted as follows. Within each group, 95% confidence intervals of the mean correlation were calculated by bootstrapping (resampling subjects with replacement 1000 times and each time recalculating the mean correlation). Differences between mean correlation coefficients were assessed by calculating 99% confidence intervals of differences between means and confidence intervals >0 were considered reliable.

Table 1
Size and Shape of Fos analysis windows in each region.

Region	size (pixels)	shape
Prelimbic	1300:1000	rectangle
Dorsomedial Striatum	1200:1200	rectangle
Mediodorsal Thalamus	1100:1250	rectangle
Orbitofrontal Cortex	1000:1000	rectangle
Ventral Tegmental Area	1000:1000	rectangle
Nucleus Accumbens, Core	850:850	oval
Nucleus Accumbens, Shell	400:700	rectangle
Ventral Pallidum	1300:1000	rectangle
Dorsal Raphe Nucleus	800:800	rectangle
Bed Nucleus of the Stria Terminalis, Lateral Ventral	700:400	rectangle
Lateral Habenula	1000:1000	rectangle
Basolateral Amygdala	1200:1200	oval
Medial Preoptic Area	700:1400	rectangle
Lateral Septum, Dorsal	300:700	rectangle
Lateral Septum, Ventral	700:300	rectangle
Dorsal Tennia Tecta	800:8000	rectangle
Piriform Cortex	1300:1000	rectangle
Olfactory Tubercle	1300:1000	rectangle
Anterior Cingulate Cortex	1300:1000	rectangle
Infralimbic	1300:1000	rectangle
Dorsolateral Striatum	1200:1200	rectangle
Ventromedial Hypothalamus	1000:1500	oval, rotated 35° toward midline
Lateral Hypothalamus	1000:1000	rectangle
Periaquiductal Gray	800:800	rectangle
Insular Cortex	1300:1000	rectangle
Paraventricular Nucleus of the Hypothalamus	1000:700	rectangle
Ventral Hippocampus	700:700	rectangle
Ventral Subiculum	1000:400	rectangle

2.5. Anatomical and functional network construction

An anatomical network was constructed using regions of interest as nodes and anatomical connections between them as edges. Anatomical connections were identified using ChemNetDB (Noori et al., 2017). This anatomical network was constructed for the purpose of thresholding the functional networks which are undirected. Therefore, the anatomical graph was also constructed with undirected edges, despite the directionality of the anatomical connection being known. The resulting network contained 178 edges.

Functional networks were constructed using ROIs as nodes and correlation coefficients between regions as edges. Each network was then thresholded to match the density of the anatomical network by rank ordering correlation coefficients in descending order and retaining the largest 178. Hubs were identified using degree and betweenness centrality. Degree corresponds to the number of edges that are incident to the node. Betweenness centrality is the fraction of all shortest path lengths that pass through the node. Degree and betweenness were both calculated for all nodes after thresholding each graph to match the density of the anatomical network. Additional network measures, including participation coefficients were computed and summarized in Table 1. Network analysis and visualization was conducted in Python 3.6 using the open-source packages Networkx 2.3 and Brain Connectivity Toolbox (Rubinov and Sporns, 2010). All scripts are available through Github (https://github.com/nworley01/StressNetwork).

3. Results

3.1. ES in male and female rats

Both male and female rats in the ES condition learned to turn the wheel to escape shock. Analysis of frequency requirement over 5 trial bins via two-way repeated measures ANOVA revealed a main effect of bin ($F(19, 418) = 23.35$; $p < 0.001$, Fig. 1B), but no main effect of sex ($F(1, 22) = 2.607$; $p = 0.1206$) nor interaction ($F(19, 418) = 0.8074$; $p = 0.6988$). Similarly, there was a main effect of bin on latency to escape the shock ($F(19, 418) = 4.293$; $p < 0.001$, Fig. 1C), but no main effect of sex ($F(1, 22) = 2.169$; $p = 0.1550$) nor interaction ($F(19, 418) = 0.3989$; $p = 0.9897$).

3.2. Induction of c-Fos expression in multiple brain regions following ES and IS

To determine how stressor controllability altered functional connectivity across brain networks, we quantified Fos expression elicited by exposure to ES, IS, and HC treatment in male and female rats. Among the 28 brain regions analyzed, two-way ANOVA revealed main effects of stress in all region except the vHipp, but no main effects of sex, nor interactions (Fig. 1D, see Table 2 for full statistics). No differences were

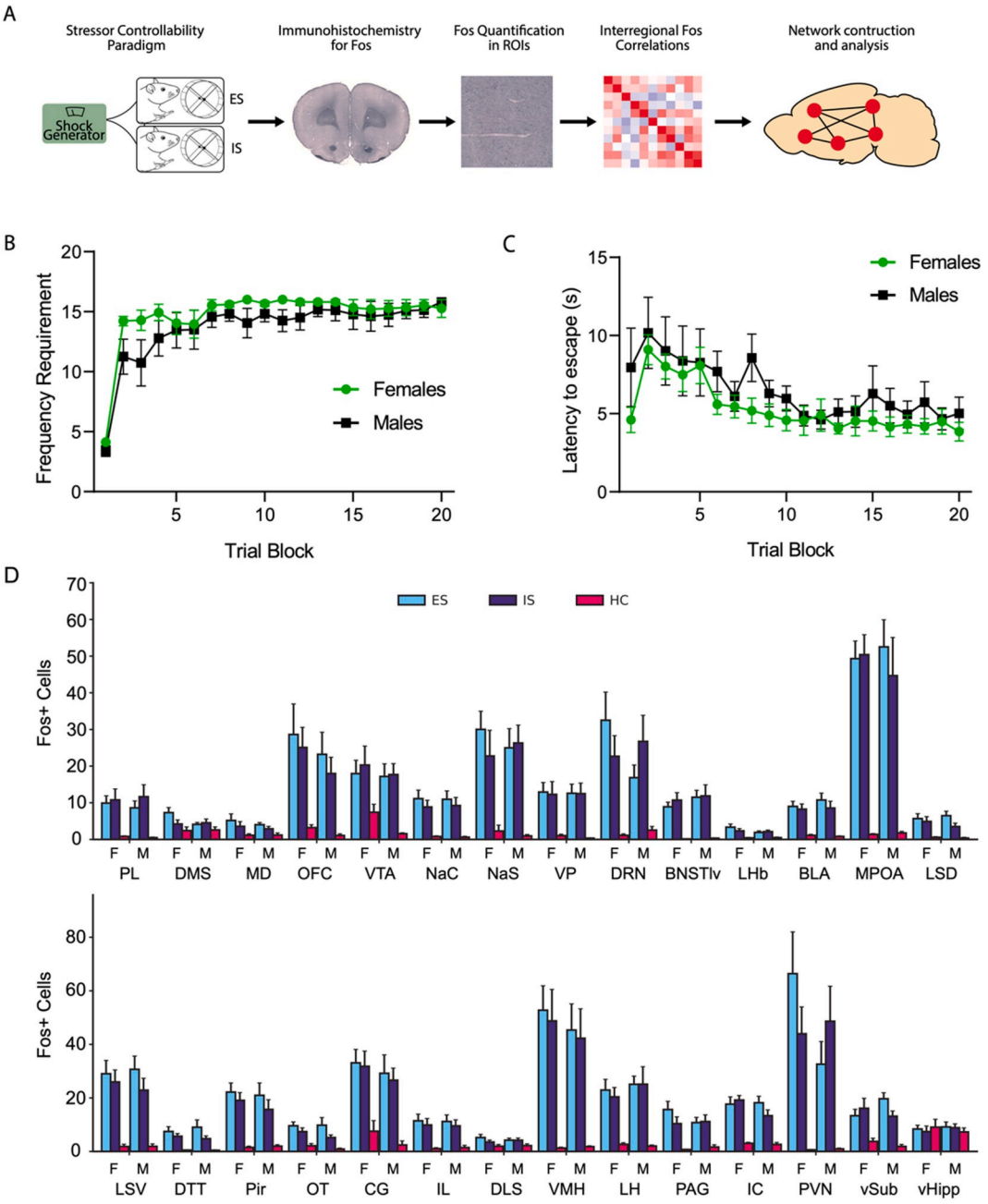

Fig. 1. Schematic of the experimental approach, wheel turn performance and regional Fos immunoreactivity. (A) Male and Female rats were exposed to ES (controllable tail shock) or IS (yoked uncontrollable tail shock). In order to quantify stress induced activity, 120 min after the end of stress brains were sectioned and stained for the immediate early gene product Fos. Fos was then quantified in 28 brain regions to produce sets of interregional correlations. Networks were constructed for each group using regions as nodes and interregional correlations as edges and used for identification of potential hubs. (B) Mean (±SEM) frequency requirement for shock termination by trial block (blocks of 5 trials) to indicate wheel turning performance of males (black squares) and females (green circles) during ES. (C) Mean (±SEM) latency to escape by trial block (blocks of 5 trails) during ES in males (black squares) and females (green circles). No sex differences were apparent in wheel turn behavior. (D) Mean (+SEM) Fos immunoreactive nuclei by ROI quantified 120min after stress treatment. Significant main effects of stress were evident in all ROIs except for ventral hippocampus (vHipp). Complete statistical results and abbreviation key are provided in Table 2. (For interpretation of the references to color in this figure legend, the reader is referred to the Web version of this article.)

found in mean Fos between ES and IS in any of the regions measured.

3.3. Functional connectivity

To determine if functional connectivity differed between groups, we compared mean r values between the stress groups: male ES, female ES, male IS, and female IS. Averaged across all brain regions, we found more correlated activity in IS females than ES females, ES males, and IS males (Fig. 2B). Surprisingly, we found correlated activity in the action-outcome network to be higher in the female IS group than the males IS group. Correlated activity in the action-outcome network did not differ between ES males and IS males (Fig. 2C). We found that correlated activity in the a priori defined stress network was lower in in the male ES group than all other groups (Fig. 2D). Connectivity between the stress network and the action-outcome network was higher in IS females in than all other groups.

Table 2
Summary of ANOVA performed on Fos counts in each brain region.

Region	Abbreviation	Main Effect of Stress	Main Effect of Sex	Interaction
Prelimbic	PL	F (2, 63) = 13.06, p < 0.0001	F (1, 63) = 0.021, p = 0.89	F (2, 63) = 0.13, p = 0.88
Dorsomedial Striatum	DMS	F (2, 59) = 4.87, p = 0.011	F (1, 59) = 1.15, p = 0.29	F (2, 59) = 1.94, p = 0.15
Mediodorsal Thalamus	MD	F (2, 63) = 5.39, p = 0.007	F (1, 63) = 0.47, p = 0.49	F (2, 63) = 0.16, p = 0.85
Orbitofrontal Cortex	OFC	F (2, 64) = 12.17, p < 0.0001	F (1, 64) = 0.00, p = 0.99	F (2, 64) = 0.00, p = 0.99
Ventral Tegmental Area	VTA	F (2, 59) = 10.39, p < 0.0001	F (1, 59) = 1.17, p = 0.28	F (2, 59) = 0.26, p = 0.77
Nucleus Accumbens, Core	NaC	F (2, 63) = 17.50, p < 0.0001	F (1, 63) = 0.00, p = 0.99	F (2, 63) = 0.017, p = 0.98
Nucleus Accumbens, Shell	NaS	F (2, 61) = 14.15, p < 0.0001	F (1, 61) = 0.083, p = 0.77	F (2, 61) = 0.18, p = 0.84
Ventral Pallidum	VP	F (2, 64) = 15.16, p < 0.0001	F (1, 64) = 0.019, p = 0.89	F (2, 64) = 0.017, p = 0.98
Dorsal Raphe Nucleus	DRN	F (2, 64) = 12.31, p < 0.0001	F (1, 64) = 0.63, p = 0.43	F (2, 64) = 2.14, p = 0.13
Bed Nucleus of the Stria Terminalis, Lateral Ventral	BNSTlv	F (2, 64) = 21.66, p < 0.0001	F (1, 64) = 0.78, p = 0.78	F (2, 64) = 0.22, p = 0.80
Lateral Habenula	LHb	F (2, 63) = 9.46, p = 0.0003	F (1, 63) = 1.54, p = 0.22	F (2, 63) = 1.16, p = 0.32
Basolateral Amygdala	BLA	F (2, 63) = 22.80, p < 0.0001	F (1, 63) = 0.26, p = 0.61	F (2, 63) = 0.28, p = 0.76
Medial Preoptic Area	MPOA	F (2, 64) = 38.39, p < 0.0001	F (1, 64) = 0.02, p = 0.88	F (2, 64) = 0.28, p = 0.76
Lateral Septum, Dorsal	LSD	F (2, 61) = 15.89, p < 0.0001	F (1, 61) = 0.08, p = 0.78	F (2, 61) = 0.65, p = 0.53
Lateral Septum, Ventral	LSV	F (2, 61) = 26.52, p < 0.0001	F (1, 61) = 0.033, p = 0.86	F (2, 61) = 0.45, p = 0.64
Dorsal Tennia Tecta	DTT	F (2, 63) = 12.99, p < 0.0001	F (1, 63) = 0.025, p = 0.87	F (2, 63) = 0.35, p = 0.71
Piriform Cortex	Pir	F (2,60) = 0.25, p < 0.0001	F (1,60) = 0.27, p = 0.60	F (2,60) = 40.35, p = 0.88
Olfactory Tubercle	OT	F (2, 64) = 13.26, p < 0.0001	F (1, 64) = 0.68, p = 0.41	F (2, 64) = 0.31, p = 0.74
Anterior Cingulate Cortex	CG	F (2, 66) = 21.64, p < 0.0001	F (1, 66) = 0.90, p = 0.35	F (2, 66) = 0.14, p = 0.87
Infralimbic	IL	F (2, 63) = 13.66, p < 0.0001	F (1, 63) = 0.001, p = 0.97	F (2, 63) = 0.02, p = 0.98
Dorsolateral Striatum	DLS	F (2, 59) = 5.00, p = 0.01	F (1, 59) = 0.0019, p = 0.97	F (2, 59) = 0.55, p = 0.58
Ventromedial Hypothalamus	VMH	F (2, 57) = 18.92, p < 0.0001	F (1, 57) = 0.40, p = 0.53	F (2, 57) = 0.13, p = 0.88
Lateral Hypothalamus	LH	F (2, 64) = 19.97, p < 0.0001	F (1, 64) = 0.45, p = 0.50	F (2, 64) = 0.25, p = 0.78
Periaquiductal Gray	PAG	F (2, 64) = 16.59, p < 0.0001	F (1, 64) = 0.35, p = 0.55	F (2, 64) = 1.18, p = 0.32
Insular Cortex	IC	F (2, 61) = 21.33, p < 0.0001	F (1, 61) = 0.64, p = 0.43	F (2, 61) = 3.12, p = 0.052
Paraventricular Nucleus of the Hypothalamus	PVN	F (2, 63) = 14.44, P < 0.0001	F (1, 63) = 1.38, p = 0.25	F (2, 63) = 2.23, p = 0.16
Ventral Hippocampus	vHipp	F (2, 50) = 0.074, p = 0.93	F (1, 50) = 0.0097, p = 0.92	F (2, 50) = 0.36, p = 0.70
Ventral Subiculum	vSub	F (2, 50) = 18.33, p < 0.0001	F (1, 50) = 0.070, p = 0.80	F (2, 50) = 2.60, p = 0.084

Table 3
Summary of significant pairwise ROI by ROI comparisons.

ROI vs ROI	Contrast
PVN vs IL	MES > FES
LHb vs DMS	FIS > MES
LSD vs DRN	FIS > MES
IL vs DMS	FIS > MES
IC vs DMS	FIS > MES
IC vs PL	FIS > MES, FIS > MIS
PAG vs PL	FIS > MIS
IC vs IL	FIS > MIS
IC vs PAG	FIS > MIS

3.4. Network analysis

An anatomical network graph was constructed with existing neuroanatomy data collected from ChemNetDB. This graph served as a template for the graphs generated with current data such that graphs in each condition could be thresholded to have the same number of edges found in the anatomical network to maintain equal network density. Nodes in the anatomy graph represent the predetermined regions of interest while edges represent anatomical connections between regions. Functional connectivity network graphs were generated using the 28 ROIs of Fos measurements as nodes and Pearson correlation coefficients as edges. For each group, networks were constructed by arranging the correlations in ascending order by p-values and adding the edges to the network sequentially until the network density matched that of the anatomical network (Fig. 3A.) or thresholded to greater than r = 0.73 (see Fig. 4).

To identify potential hubs within each of the networks all nodes were ranked according to degree (Fig. 3B) and betweenness centrality (Fig. 3C). Nodes with degree or betweenness centrality measures greater than two standard deviations above the mean were considered to be

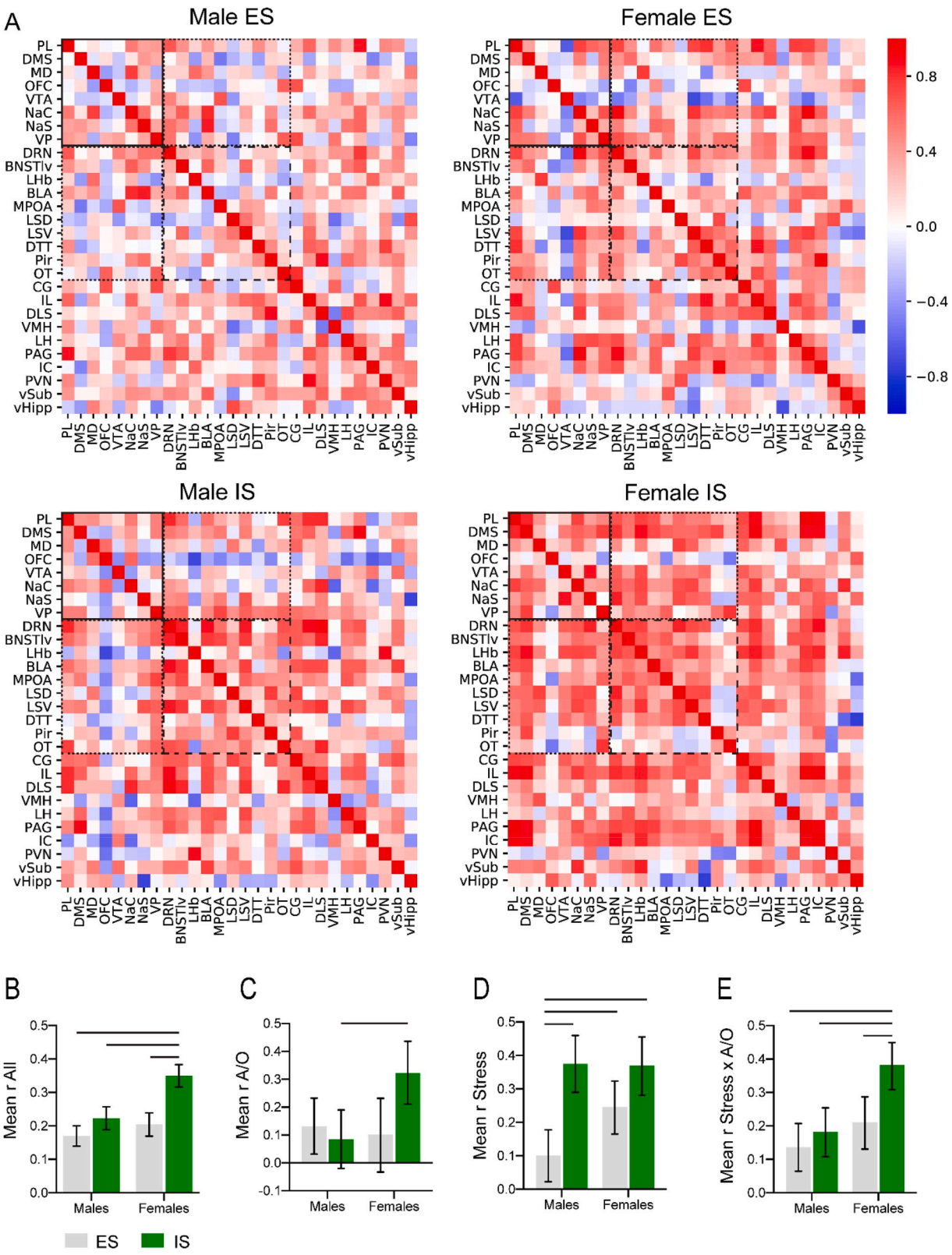

Fig. 2. Analysis of interregional Fos correlations. (A) Correlation matrix indicating functional correlations (Pearson's r) among ROIs; separate plots are provided for each treatment condition. The solid box denotes correlations within the a priori defined action/outcome (A/O) network, the dashed box denotes correlations within the a priori defined stress network, and the dotted box denotes correlations between A/O and stress regions. ROI abbreviations can be found in Table 2. Color depicts correlation strength (Pearson's r) indicated by the scale bar on the right. Positive correlations are red and negative correlations are blue. (B) Mean r value across all regions of interest per group. (C) Mean r value in A/O associated regions per group. (D) Mean r value across A/O associated regions per group. (E) Mean r value across stress associated regions per group. Overhead lines represent significant differences between groups determined by 99% confidence of difference between means. All error bars represent bootstrapped 95% confidence intervals of the mean. (For interpretation of the references to color in this figure legend, the reader is referred to the Web version of this article.)

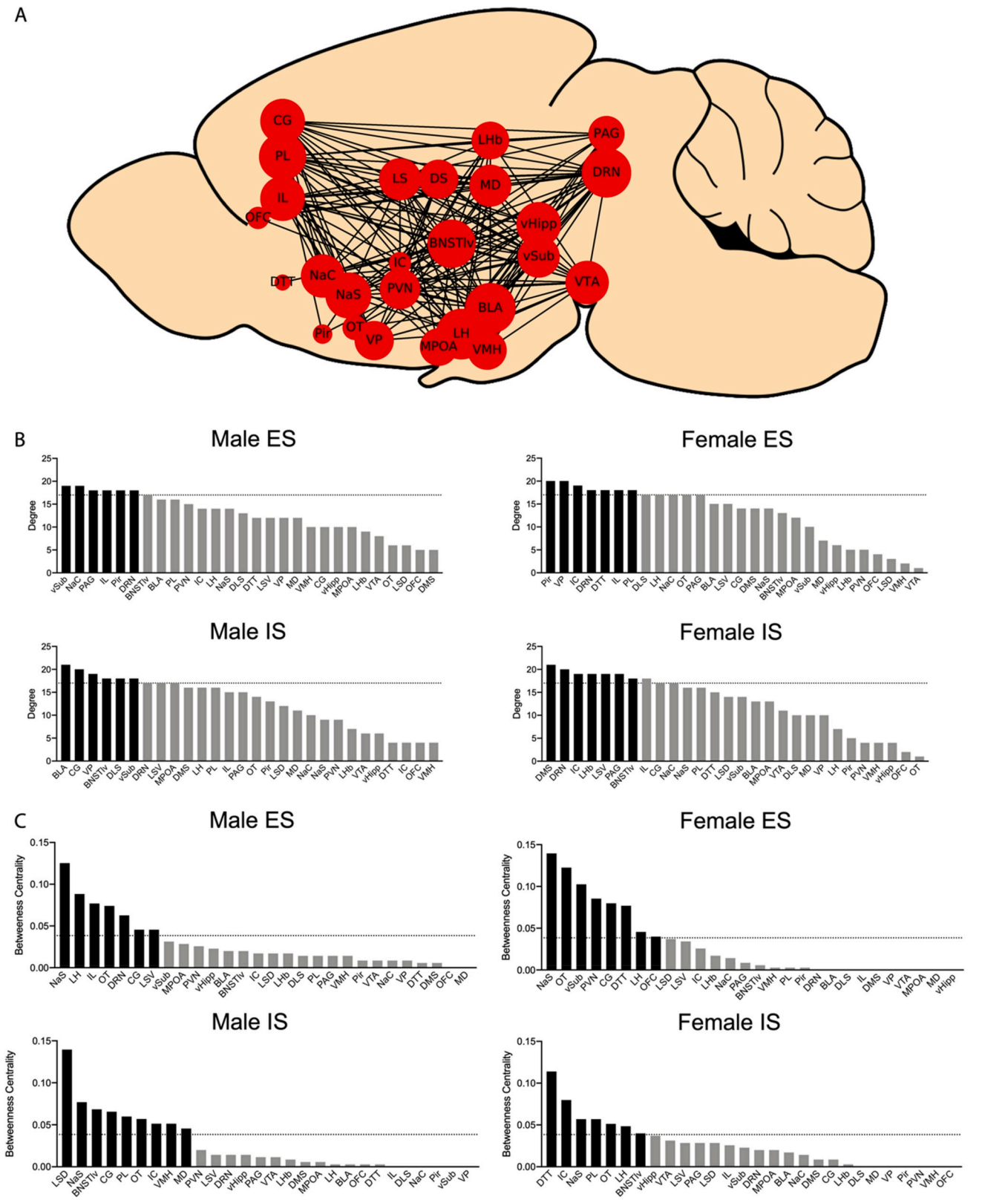

Fig. 3. Graph based analysis of hub measures in functional networks. (A) Sagittal view schematic representing a network containing nodes (red circles) of 28 regions of interest and edges (black lines) of their anatomical connections in the rat brain. The circle size for each ROI represents the anatomical node degree. (B) Degree scores based on thresholded functional connectivity networks for all regions of interest per group. Black bars depict regions greater than 2 standard deviations above mean degree (dashed lines) in random networks of equal density. (D) Betweenness centrality scores for all regions of interest per group. Black bars depict regions greater than 2 standard deviations above mean betweenness centrality (dashed lines) in random networks of equal density. (For interpretation of the references to color in this figure legend, the reader is referred to the Web version of this article.)

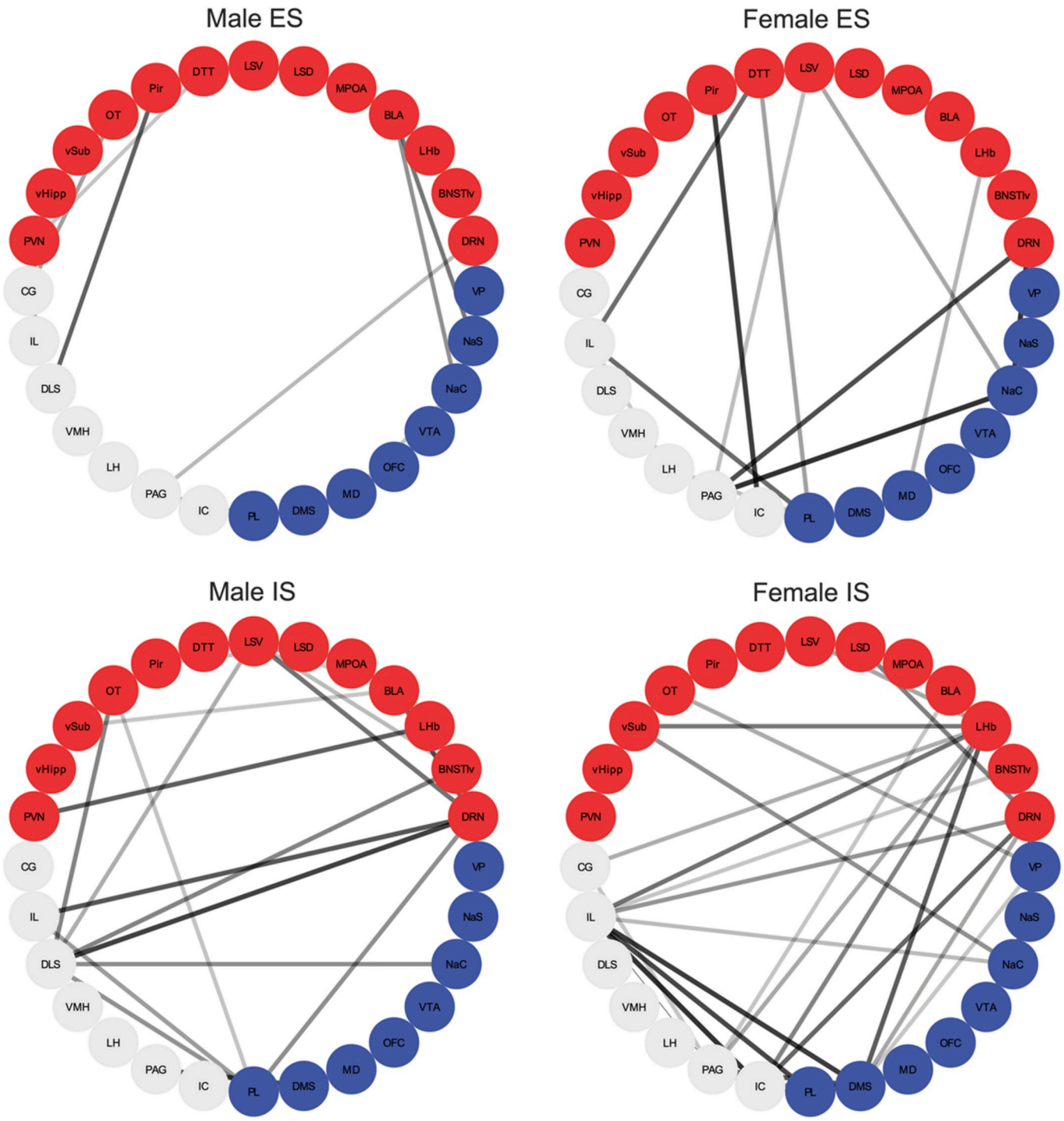

Fig. 4. Network visualization of nodes for male and female stress conditions. Nodes are organized by a priori network (red = stress, blue = A/O, gray = other). Edges were included for interregional correlations greater than r = 0.73, corresponding to a power>0.8, in for Male ES, Female ES, Male IS, and Female IS. Greater line width and opacity correspond with greater r values.

potential hubs. In the male ES condition, the vSub, NaC, PAG, IL, Pir, and DRN represent potential hubs based on degree, while the NaS, LH, IL, OT, DRN, CG, and LSV represent potential hubs based on betweenness centrality. In the female ES condition Pir, VP, IC, DRN, DTT, IL, and PL represent potential hubs based on degree, while the NaS, OT, vSub, PVN, CG, DTT, LH, and OF represent potential hubs based on betweenness centrality. In the males IS condition the BLA, CG, VP, BNSTlv, DLS, vSub emerged as potential hubs based on degree, and the LSD. NaS, BNSTlv, CG, PL, OT, IC, VMH, MD emerged as potential hubs based on betweenness centrality. Finally, in the female IS condition, the DMS, DRN, IC, LHb, LSV, PAG, BNSTlv were identified as potential hubs based on degree, and the DTT, IC, NAS, PL, OT, LH, BNSTlv represent potential hubs based on betweenness centrality.

4. Discussion

We investigated how stressor controllability alters functional connectivity in stress- and action/outcome-associated brain areas in male

and female rats. Similar to the finding of Baratta et al. (2018), no sex differences were observed in rate of learning to wheel-turn to escape a tail-shock stressor. Although in many cases stress itself raised Fos counts, we found no differences in the number of Fos cells in any brain regions regardless of sex or stressor controllability. However, sex and stressor controllability differences emerged when we looked at brain network connectivity through interregional correlations. Network analyses revealed potential hub nodes based on degree and betweenness for male ES (IL and DRN), male IS (CG, BNSTlv), female ES (IC), and female IS (IC). The key take-away from these analyses is that greater connectivity across brain regions was common to the stress treatments previously shown to induce anxiety, females with ES, and males and females with IS. In each condition a varied set of functionally connected ROIs were identified opening the way for a more systematic view of neural activity in the face of traumatic stress.

We are not the first to investigate stress-induced Fos activity to probe brain regions engaged during coping, and that neither controllability of stress nor sex influenced the mean Fos expression in any ROI is consistent with other investigations of neural activation following ES and IS (Baratta et al., 2009; Dolzani et al., 2016; Grahn et al., 1999; Weinberg et al., 2010). In prior studies, differences resulting from controllability were apparent only when Fos was quantified within cell specific populations, identified by neurotransmitter (Grahn et al., 1999) or anatomical projections (Baratta et al., 2009). However, some exceptions are worth consideration. First, in the DMS, ES induced greater Fos compared to IS (Amat et al., 2014). Surprisingly, we did not find controllability differences in the same region, but this may be related to procedural differences including the housing of males and females within the same vivarium, immunohistochemistry protocols or antibodies used. Second, Kim and colleagues (Kim et al., 2016) measured Fos in Fos-GFP reporter mice behaviorally categorized as stress-resistant or stress-susceptible. They first exposed mice to 2 sessions of 360 inescapable, uncontrollable foot shock stress followed by a test session consisting of a shuttle-box escape to evaluate “resilient” versus “helpless” mice. In contrast to the current findings, brain-wide analysis of the Fos-GFP reporter after the test session revealed that helpless mice showed a nearly global reduction in stress-induced Fos activity compared with resilient mice. This is interesting because the susceptible mice received quantitatively more shock exposure because they repeatedly failed to escape in the shuttlebox test. While differences in findings may be attributed species differences (Sprague-Dawley rat vs, knock-in mice), method of Fos quantification (IHC vs. genetic Fos reporter), or differences in stress procedures (100 tailshocks vs. 360 footshocks followed by shuttle box tests), they might alternatively suggest that difference in neuronal activation among stress resilient and stress susceptible individuals as measured by Fos cannot be resolved during the initial stressor, but only upon subsequent stress exposure. This is the first study to look at sex differences across these regions in the stressor controllability paradigm; that no sex differences in total Fos were apparent was unexpected, but may reflect the need to identify cell types to resolve differences in individual regions or obscured by the blunt temporal resolution of Fos as an endpoint measure.

We found that functional connectivity changes as a result of stressor controllability and sex in a number of ways. First, females in the IS condition have higher mean Pearson’s r among all ROIs than all other groups, and this effect is mirrored in stress by action-outcome regions. This suggests females may have increased coordination within, or increased demand upon, these brain networks. Second, IS in females resulted in higher mean Pearson’s r among action-outcome regions than male IS. This sex difference after exposure to IS may reflect increased coordination within these brain networks in females. Third, as predicted, ES in males resulted in lower functional connectivity in the stress network suggesting that control over stress disrupted or inhibited activity in the network mediating stress response. Fourth, although we predicted that after ES there would be increased functional connectivity between the stress network and the action-outcome network, we found little functional connectivity in the ES groups but high connectivity between these two networks in IS females.

The greater functional connectivity observed in the IS conditions and the female ES condition may reflect how neural systems are recruited to cope with the stressor over time. At the initiation of the stress exposure, both ES and IS rats are exposed to an identical tail shock which likely similarly engages coordinated activation among stress circuitry. In the first ~25 trials, ES rats are learning to turn the wheel to terminate the shock, which presumably engages action-outcome circuitry and disengages stress circuitry. In fact, some of the effects of ES, including the blunting of DRN 5-HT release and plasticity, are evident in 15–25 trials (Amat et al., 1998; Christianson et al., 2014). The lack of observed functional connectivity in the male ES action-outcome network here, then, may be the result of the brief activation that was not detectable by Fos. On the other hand, IS rats, unable to escape tail shock, learn no such contingency, requiring sustained stress response. Over time, IS rats may attempt numerous coping strategies that may recruit and sustain drive to a broader circuitry.

The surprising finding that the highest functional connectivity in action-outcome regions occurred in females after IS may reflect sex differences in networks required to mediate the behavioral strategies used during stress. Several lines of preclinical work demonstrate sex differences in the physiological and behavioral responses to stress (Drossopoulou et al., 2004; Rincón-Cortés and Grace, 2017; Wiersielis et al., 2016). Several studies in humans also provide evidence of sex differences in functional brain networks using resting-state functional connectivity MRI (Ghahramani et al., 2014). However, an analogous “resting-state” functional connectivity network in rodent couldn’t be constructed with data from the HC animals, as Fos was not detected across the majority of brain regions observed. Furthermore, numerous studies in rats have shown sex differences in behavioral strategies following stress, including females showing darting response during fear conditioning and subsequently increased fear generalization (reviewed in Shansky, 2018). Although tail-restrained in the current paradigm, the female IS rats may be attempting to engage in a more active coping strategy.

Applying network analysis to this type of data allowed for the identification of potential hub regions - using measures of degree, betweenness, and participations coefficient – that are believed to play a disproportionate role within the network (Rubinov and Sporns, 2010). Our analysis reveals that a number of regions may play important roles in under certain stress conditions and warrant further investigation. For example, the BNSTlv emerged as a likely hub in both stress conditions in males and in the female IS condition and represents a node of high degree and participation coefficient in IS. Indeed, the BNSTlv is active following IS (Christianson et al., 2011) and is required for the potentiation of fear conditioning, shuttle-box escape deficit, and reduced social exploration following IS (Christianson et al., 2009; Hammack et al., 2004). The BNSTlv is highly interconnected with many limbic structures including the prefrontal cortex, hippocampus, and amygdala (Dong et al., 2001; Dong and Swanson, 2004) as well as the DRN (Dong and Swanson, 2004; Shin et al., 2008) and therefore well positioned to exert influence over stress. This example highlights the need for future investigation into the role BNSTlv plays in stress coping. Similarly, the other hubs we identified in this work, including IC, IL, NaS, and OT, are also important sites for future investigation.

The goal of a Fos-based functional connectivity approach is to understand, broadly, the network structure and identify targets for further inquiry. In the current data, this analysis detected robust connectivity within known nodes of stress networks but did not capture the expected connectivity within the action-outcome network. This failure may reflect something true about the nature of functional connectivity in stressor controllability, or it may be a consequence of the limitations of the Fos-based analysis. First, examination of Fos alone is not cell type nor projection specific, thus group differences in activation of specific cell types, such as DRN 5-HT neurons (Grahn et al., 1999), or group

differences in cells with specific projections, such as PL projections to the DRN (Baratta et al., 2009), cannot be resolved. Second, analysis of Fos doesn't capture the temporal specificity of complex cell firing that likely occurs over the 2 h stress exposure. Correlated activation between regions early during the stress exposure may become occluded by activity patterns in this network present later in the stress exposure. However, that we did not find evidence to support our prediction that high interregional correlations between regions of the action-outcome network in ES males does not eliminate the possibility that high functional connectivity occurred within this network at some point during the stress exposure.

To conclude, these results add to a body of literature showing that neural activity is impacted by sex and stressor controllability. Uncontrollable stress, and controllable stress in females, was associated with higher functional connectivity within the stress network. In males, ES may interrupt connectivity within the stress network, but in females, under these experimental conditions control over stress doesn't appear to disrupt the stress network or protect against stress induced anxiety (Baratta et al., 2018). Our results supplement prior work showing sex differences in networks activated by stress. These results further highlight the importance of a number of structures to specific networks, including the BNSTlv, IC, and IL, which represent promising avenues for exploring their role in stress and controllability. Future work seeking to prevent stress induced behavioral changes should focus on means of disrupting the stress network, potentially through pharmacological or neurofeedback approaches, and further investigate sex differences in networks activated by stress, and elucidate the roles of newly identified hubs in this paradigm.

CRediT authorship contribution statement

N.B. Worley: Conceptualization, Methodology, Investigation, Software, Formal analysis, Writing - original draft, Visualization, Writing - review & editing. **S.R. Everett:** Investigation, Writing - review & editing. **A.R. Foilb:** Methodology, Investigation, Writing - review & editing. **J.P. Christianson:** Conceptualization, Funding acquisition, Writing - review & editing, Supervision.

Acknowledgements

Funding for this work was provided by the NIH Grant MH110907 and the Gianinno Family to JPC. The authors have no competing financial or other conflicts of interest to declare. We thank Bret Judson and the Boston College Imaging Core for infrastructure and support. Nancy McGilloway and Todd Gaines oversaw animal husbandry in the Boston College Animal Care Facility.

References

Amat, J., Baratta, M.V., Paul, E., Bland, S.T., Watkins, L.R., Maier, S.F., 2005. Medial prefrontal cortex determines how stressor controllability affects behavior and dorsal raphe nucleus. Nat. Neurosci. 8, 365–371. https://doi.org/10.1038/nn1399.

Amat, J., Christianson, J.P., Aleksejev, R.M., Kim, J., Richeson, K.R., Watkins, L.R., Maier, S.F., 2014. Control over a stressor involves the posterior dorsal striatum and the act/outcome circuit. Eur. J. Neurosci. 40, 2352–2358. https://doi.org/10.1111/ejn.12609.

Amat, J., Matus-Amat, P., Watkins, L.R., Maier, S.F., 1998. Escapable and inescapable stress differentially alter extracellular levels of 5-HT in the basolateral amygdala of the rat. Brain Res. 812, 113–120. https://doi.org/10.1016/S0006-8993(98)00960-3.

Balleine, B.W., Dickinson, A., 1998. Goal-directed instrumental action: contingency and incentive learning and their cortical substrates. Neuropharmacology 37, 407–419. https://doi.org/10.1016/S0028-3908(98)00033-1.

Balleine, B.W., O'Doherty, J.P., 2010. Human and rodent homologies in action control: corticostriatal determinants of goal-directed and habitual action. Neuropsychopharmacology 35, 48–69. https://doi.org/10.1038/npp.2009.131.

Baratta, M.V., Gruene, T.M., Dolzani, S.D., Chun, L.E., Maier, S.F., Shansky, R.M., 2019. Controllable stress elicits circuit-specific patterns of prefrontal plasticity in males, but not females. Brain Struct. Funct. https://doi.org/10.1007/s00429-019-01875-z.

Baratta, M.V., Leslie, N.R., Fallon, I.P., Dolzani, S.D., Chun, L.E., Tamalunas, A.M., Watkins, L.R., Maier, S.F., 2018. Behavioural and neural sequelae of stressor exposure are not modulated by controllability in females. Eur. J. Neurosci. 47, 959–967. https://doi.org/10.1111/ejn.13833.

Baratta, M.V., Zarza, C.M., Gomez, D.M., Campeau, S., Watkins, L.R., Maier, S.F., 2009. Selective activation of dorsal raphe nucleus-projecting neurons in the ventral medial prefrontal cortex by controllable stress. Eur. J. Neurosci. 30, 1111–1116. https://doi.org/10.1111/j.1460-9568.2009.06867.x.

Benjamini, Y., Hochberg, Y., 1995. Controlling the false discovery Rate : a practical and powerful approach to multiple testing. J. Roy. Stat. Soc. 57, 289–300.

Breslau, Naomi, 2002. Epidemiologic studies of trauma, posttraumatic stress disorder, and other psychiatric disorders. Can. J. Psychiatr. 47, 923–929.

Breslau, N., Davis, G., 1992. Posttraumatic stress disorder in an urban population of young adults: risk factors for chronicity. Am. J. Psychiatr. 149, 671–675. https://doi.org/10.1176/ajp.149.5.671.

Christianson, J.P., Flyer-Adams, J.G., Drugan, R.C., Amat, J., Daut, R.A., Foilb, A.R., Watkins, L.R., Maier, S.F., 2014. Learned stressor resistance requires extracellular signal-regulated kinase in the prefrontal cortex. Front. Behav. Neurosci. 8, 1–11. https://doi.org/10.3389/fnbeh.2014.00348.

Christianson, J.P., Greenwood, B.N., 2014. Stress-protective neural circuits: not all roads lead through the prefrontal cortex. Stress 17, 1–12. https://doi.org/10.3109/10253890.2013.794450.

Christianson, J.P., Jennings, J.H., Ragole, T., Flyer, J.G.N., Benison, A.M., Barth, D.S., Watkins, L.R., Maier, S.F., 2011. Safety signals mitigate the consequences of uncontrollable stress via a circuit involving the sensory insular cortex and bed nucleus of the stria terminalis. Biol. Psychiatr. 70, 458–464. https://doi.org/10.1016/j.biopsych.2011.04.004.

Christianson, J.P., Paul, E.D., Irani, M., Thompson, B.M., Kubala, K.H., Yirmiya, R., Watkins, L.R., Maier, S.F., 2008. The role of prior stressor controllability and the dorsal raphé nucleus in sucrose preference and social exploration. Behav. Brain Res. 193, 87–93. https://doi.org/10.1016/j.bbr.2008.04.024.

Christianson, J.P., Ragole, T., Amat, J., Greenwood, B.N., Strong, P.V., Paul, E.D., Fleshner, M., Watkins, L.R., Maier, S.F., 2010. 5-Hydroxytryptamine 2C receptors in the basolateral amygdala are involved in the expression of anxiety after uncontrollable traumatic stress. Biol. Psychiatr. 67, 339–345. https://doi.org/10.1016/j.biopsych.2009.09.011.

Christianson, J.P., Thompson, B.M., Watkins, L.R., Maier, S.F., 2009. Medial prefrontal cortical activation modulates the impact of controllable and uncontrollable stressor exposure on a social exploration test of anxiety in the rat. Stress 12, 445–450. https://doi.org/10.1080/10253890802510302.

Coco, M.L., Weiss, J.M., 2005. Neural substrates of coping behavior in the rat: possible importance of mesocorticolimbic dopamine system. Behav. Neurosci. 119, 429–445. https://doi.org/10.1037/0735-7044.119.2.429.

Corbit, L.H., Balleine, B.W., 2003. The role of prelimbic cortex in instrumental conditioning. Behav. Brain Res. 146, 145–157. https://doi.org/10.1016/j.bbr.2003.09.023.

Dolzani, S.D., Baratta, M.V., Amat, J., Agster, K.L., Saddoris, M.P., Watkins, L.R., Maier, S.F., 2016. Activation of a habenulo-raphe circuit is critical for the behavioral and neurochemical consequences of uncontrollable stress in the male rat. eNeuro 3, 1–17. https://doi.org/10.1523/ENEURO.0229-16.2016.

Dong, H.W., Petrovich, G.D., Watts, A.G., Swanson, L.W., 2001. Basic organization of projections from the oval and fusiform nuclei of the bed nuclei of the stria terminalis in adult rat brain. J. Comp. Neurol. 436, 430–455. https://doi.org/10.1002/cne.1079.

Dong, H.W., Swanson, L.W., 2004. Organization of axonal projections from the anterolateral area of the bed nuclei of the stria terminalis. J. Comp. Neurol. 468, 277–298. https://doi.org/10.1002/cne.10949.

Drossopoulou, G., Antoniou, K., Kitraki, E., Papathanasiou, G., Papalexi, E., Dalla, C., Papadopoulou-Daifoti, Z., 2004. Sex differences in behavioral, neurochemical and neuroendocrine effects induced by the forced swim test in rats. Neuroscience 126, 849–857. https://doi.org/10.1016/j.neuroscience.2004.04.044.

Ghahramani, N.M., Ngun, T.C., Chen, P.-Y., Tian, Y., Krishnan, S., Muir, S., Rubbi, L., Arnold, A.P., de Vries, G.J., Forger, N.G., Pellegrini, M., Vilain, E., 2014. The effects of perinatal testosterone exposure on the DNA methylome of the mouse brain are late-emerging. Biol. Sex Differ. 5, 8. https://doi.org/10.1186/2042-6410-5-8.

Gillikin, C., Habib, L., Evces, M., Bradley, B., Ressler, K.J., Sanders, J., 2016. Trauma exposure and PTSD symptoms associate with violence in inner city civilians. J. Psychiatr. Res. 83, 1–7. https://doi.org/10.1016/j.jpsychires.2016.07.027.

Grahn, R.E., Will, M.J., Hammack, S.E., Maswood, S., McQueen, M.B., Watkins, L.R., Maier, S.F., 1999. Activation of serotonin-immunoreactive cells in the dorsal raphe nucleus in rats exposed to an uncontrollable stressor. Brain Res. 826, 35–43. https://doi.org/10.1016/S0006-8993(99)01208-1.

Hammack, S.E., Richey, K.J., Watkins, L.R., Maier, S.F., 2004. Chemical lesion of the bed nucleus of the stria terminalis blocks the behavioral consequences of uncontrollable stress. Behav. Neurosci. https://doi.org/10.1037/0735-7044.118.2.443.

Hart, G., Bradfield, L.A., Balleine, B.W., 2018. Prefrontal cortico-striatal disconnection blocks the acquisition of goal-directed action. J. Neurosci. 38 https://doi.org/10.1523/JNEUROSCI.2850-17.2017, 2850–17.

Herbison, C.E., Allen, K., Robinson, M., Newnham, J., Pennell, C., 2017. The impact of life stress on adult depression and anxiety is dependent on gender and timing of exposure. Dev. Psychopathol. 29, 1443–1454. https://doi.org/10.1017/S0954579417000372.

Kim, Y., Perova, Z., Mirrione, M.M., Pradhan, K., Henn, F.A., Shea, S., Osten, P., Li, B., 2016. Whole-brain mapping of neuronal activity in the learned helplessness model of depression. Front. Neural Circ. 10, 1–11. https://doi.org/10.3389/fncir.2016.00003.

Leuner, B., Mendolia-Loffredo, S., Shors, T.J., 2004. Males and females respond differently to controllability and antidepressant treatment. Biol. Psychiatr. 56, 964–970. https://doi.org/10.1016/j.biopsych.2004.09.018.

Machida, M., Lonart, G., Sanford, L.D., 2018. Effects of stressor controllability on transcriptional levels of c-fos, Arc, and brain-derived neurotrophic factor in mouse amygdala and medial prefrontal cortex. Neuroreport 29, 112–117. https://doi.org/10.1097/WNR.0000000000000919.

Maier, S.F., 1990. Role of fear in mediating shuttle escape learning deficit produced by inescapable shock. J. Exp. Psychol. Anim. Behav. Process. https://doi.org/10.1037/0097-7403.16.2.137.

Maier, S.F., Kalman, B.A., Grahn, R.E., 1994. Chlordiazepoxide microinjected into the region of the dorsal raphe nucleus eliminates the interference with escape responding produced by inescapable shock whether administered before inescapable shock or escape testing. Behav. Neurosci. https://doi.org/10.1037/0735-7044.108.1.121.

Maier, S.F., Seligman, M.E.P., 2016. Learned helplessness at fifty: insights from neuroscience. Psychol. Rev. 123, 349–367. https://doi.org/10.1037/rev0000033.

Maier, S.F., Watkins, L.R., 2010. Role of the medial prefrontal cortex in coping and resilience. Brain Res. 1355, 52–60. https://doi.org/10.1016/j.brainres.2010.08.039.

Maier, S.F., Watkins, L.R., 2005. Stressor controllability and learned helplessness: the roles of the dorsal raphe nucleus, serotonin, and corticotropin-releasing factor. Neurosci. Biobehav. Rev. 29, 829–841. https://doi.org/10.1016/j.neubiorev.2005.03.021.

McReynolds, J.R., Christianson, J.P., Blacktop, J.M., Mantsch, J.R., 2018. Neurobiology of Stress What does the Fos say? Using Fos-based approaches to understand the contribution of stress to substance use disorders. Neurobiol. Stress 9, 271–285. https://doi.org/10.1016/j.ynstr.2018.05.004.

Noori, H.R., Schöttler, J., Ercsey-Ravasz, M., Cosa-Linan, A., Varga, M., Toroczkai, Z., Spanagel, R., 2017. A multiscale cerebral neurochemical connectome of the rat brain. PLoS Biol. 15, 1–23. https://doi.org/10.1371/journal.pbio.2002612.

Paxinos, George, Watson, Charles, 2007. The Rat Brain in Stereotaxic Coordinates., 6th. Academic Press, London.

Rincón-Cortés, M., Grace, A.A., 2017. Sex-dependent effects of stress on immobility behavior and VTA dopamine neuron activity: modulation by ketamine. Int. J. Neuropsychopharmacol. 20, 823–832. https://doi.org/10.1093/ijnp/pyx048.

Rogers-Carter, M.M., Varela, J.A., Gribbons, K.B., Pierce, A.F., Morgan, M.T.M., Ritchey, M., Christianson, J.P., 2018. Insular cortex mediates approach and avoidance responses to social affective stimuli. https://doi.org/10.1038/nm.2451.A.

Rubinov, M., Sporns, O., 2010. Complex network measures of brain connectivity: uses and interpretations. Neuroimage 52, 1059–1069. https://doi.org/10.1016/j.neuroimage.2009.10.003.

Shansky, R.M., 2018. Sex differences in behavioral strategies: avoiding interpretational pitfalls. Curr. Opin. Neurobiol. 49, 95–98. https://doi.org/10.1016/j.conb.2018.01.007.

Shin, J.-W., Geerling, J.C., Loewy, A.D., 2008. Inputs to the ventrolateral bed nucleus of the stria terminalis. J. Comp. Neurol. 511, 628–657. https://doi.org/10.1002/cne.21870.

Short, K.R., Maier, S.F., 1993. Stressor controllability, social interaction, and benzodiazepine systems. Pharmacol. Biochem. Behav. 45, 827–835. https://doi.org/10.1016/0091-3057(93)90128-G.

Southwick, S.M., Vythilingam, M., Charney, D.S., 2005. The psychobiology of depression and resilience to stress: implications for prevention and treatment. Annu. Rev. Clin. Psychol. 1, 255–291. https://doi.org/10.1146/annurev.clinpsy.1.102803.143948.

Tanimizu, T., Kenney, J.W., Okano, E., Kadoma, K., Frankland, P.W., Kida, S., 2017. Functional connectivity of multiple brain regions required for the consolidation of social recognition memory. J. Neurosci. 37, 4103–4116. https://doi.org/10.1523/jneurosci.3451-16.2017.

Thompson, N.J., Fiorillo, D., Rothbaum, B.O., Ressler, K.J., Michopoulos, V., 2018. Coping strategies as mediators in relation to resilience and posttraumatic stress disorder. J. Affect. Disord. 225, 153–159. https://doi.org/10.1016/j.jad.2017.08.049.

Valentino, R.J., Bangasser, D.A., 2016. Sex-biased cellular signaling: molecular basis for sex differences in neuropsychiatric diseases. Dialogues Clin. Neurosci. 18, 385–393.

Weinberg, M.S., Grissom, N., Paul, E., Bhatnagar, S., Maier, S.F., Spencer, R.L., 2010. Inescapable but not escapable stress leads to increased struggling behavior and basolateral amygdala c-fos gene expression in response to subsequent novel stress challenge. Neuroscience 170, 138–148. https://doi.org/10.1016/j.neuroscience.2010.06.052.

Wheeler, A.L., Teixeira, C.M., Wang, A.H., Xiong, X., Kovacevic, N., Lerch, J.P., McIntosh, A.R., Parkinson, J., Frankland, P.W., 2013. Identification of a functional connectome for long-term fear memory in mice. PLoS Comput. Biol. 9 https://doi.org/10.1371/journal.pcbi.1002853.

Wiersielis, K.R., Wicks, B., Simko, H., Cohen, S.R., Khantsis, S., Baksh, N., Waxler, D.E., Bangasser, D.A., 2016. Sex differences in corticotropin releasing factor-evoked behavior and activated networks. Psychoneuroendocrinology 73, 204–216. https://doi.org/10.1016/j.psyneuen.2016.07.007.

Worley, N.B., Hill, M.N., Christianson, J.P., 2018. Prefrontal endocannabinoids, stress controllability and resilience: a hypothesis. Prog. Neuro-Psychopharmacol. Biol. Psychiatry 85, 180–188. https://doi.org/10.1016/j.pnpbp.2017.04.004.